



HAL
open science

Fluorinated Benzofuran and Dihydrobenzofuran as Anti-Inflammatory and Potential Anticancer Agents

Abeer J. Ayoub, Ghewa A El-Achkar, Sandra E Ghayad, Layal Hariss, Razan H. Haidar, Leen M. Antar, Zahraa I. Mallah, Bassam Badran, René Grée, Ali Hachem, et al.

► **To cite this version:**

Abeer J. Ayoub, Ghewa A El-Achkar, Sandra E Ghayad, Layal Hariss, Razan H. Haidar, et al.. Fluorinated Benzofuran and Dihydrobenzofuran as Anti-Inflammatory and Potential Anticancer Agents. International Journal of Molecular Sciences, 2023, 24 (12), pp.10399. 10.3390/ijms241210399 . hal-04164372v1

HAL Id: hal-04164372

<https://hal.science/hal-04164372v1>

Submitted on 18 Jul 2023 (v1), last revised 20 Dec 2023 (v2)

HAL is a multi-disciplinary open access archive for the deposit and dissemination of scientific research documents, whether they are published or not. The documents may come from teaching and research institutions in France or abroad, or from public or private research centers.

L'archive ouverte pluridisciplinaire **HAL**, est destinée au dépôt et à la diffusion de documents scientifiques de niveau recherche, publiés ou non, émanant des établissements d'enseignement et de recherche français ou étrangers, des laboratoires publics ou privés.



Distributed under a Creative Commons Attribution 4.0 International License



Article

Fluorinated Benzofuran and Dihydrobenzofuran as Anti-Inflammatory and Potential Anticancer Agents

Abeer J. Ayoub^{1,2,3}, Ghewa A. El-Achkar^{1,4}, Sandra E. Ghayad^{5,6}, Layal Hariss⁷, Razan H. Haidar^{1,2}, Leen M. Antar^{1,2}, Zahraa I. Mallah^{1,2}, Bassam Badran², René Grée⁸, Ali Hachem^{7,†}, Eva Hamade^{2,†} and Aida Habib^{9,*,†} 

¹ Department of Biochemistry and Molecular Genetics, Faculty of Medicine, American University of Beirut, Beirut 1107 2020, Lebanon; abeer.ayoub@liu.edu.lb (A.J.A.); gachkar@sgub.edu.lb (G.A.E.-A.); razan.haidar95@outlook.com (R.H.H.); zahraamallah@outlook.com (Z.I.M.)

² Laboratory of Cancer Biology and Molecular Immunology, Faculty of Sciences I, Lebanese University, Hadath 1104, Lebanon; bassam.badran@ul.edu.lb (B.B.); eva.hamade@ul.edu.lb (E.H.)

³ Department of Biological Sciences, School of Arts and Sciences, Lebanese International University, Bekaa Campus, Bekaa 146404, Lebanon

⁴ Faculty of Medicine, Saint George University of Beirut, Achrafieh, Beirut 1100-2807, Lebanon

⁵ Department of Biology, Faculty of Sciences II, EDST, Lebanese University, Fanar 90656, Lebanon; sandra.ghayad@univ-amu.fr

⁶ Center for CardioVascular and Nutrition Research (C2VN), INSERM 1263, INRAE 1260, Aix-Marseille University, 13385 Marseille, France

⁷ Laboratory for Medicinal Chemistry and Natural Products, Faculty of Sciences I, PRASE-EDST, Lebanese University, Hadath 1104, Lebanon; layalharis@gmail.com (L.H.); ahachem@ul.edu.lb (A.H.)

⁸ Université de Rennes, CNRS, ISCR (Institut des Sciences Chimiques de Rennes), UMR 6226, 35000 Rennes, France; rene.gree@univ-rennes1.fr

⁹ Department of Basic Medical Sciences, College of Medicine, QU Health, Qatar University, Doha 2713, Qatar

* Correspondence: aida.habib@qu.edu.qa

† These authors are senior authors and contributed equally to this work.



Citation: Ayoub, A.J.; El-Achkar, G.A.; Ghayad, S.E.; Hariss, L.; Haidar, R.H.; Antar, L.M.; Mallah, Z.I.; Badran, B.; Grée, R.; Hachem, A.; et al. Fluorinated Benzofuran and Dihydrobenzofuran as Anti-Inflammatory and Potential Anticancer Agents. *Int. J. Mol. Sci.* **2023**, *24*, 10399. <https://doi.org/10.3390/ijms241210399>

Academic Editors: Federica Finetti and Lorenza Trabalzini

Received: 19 May 2023

Revised: 15 June 2023

Accepted: 16 June 2023

Published: 20 June 2023



Copyright: © 2023 by the authors. Licensee MDPI, Basel, Switzerland. This article is an open access article distributed under the terms and conditions of the Creative Commons Attribution (CC BY) license (<https://creativecommons.org/licenses/by/4.0/>).

Abstract: Benzofuran and 2,3-dihydrobenzofuran scaffolds are heterocycles of high value in medicinal chemistry and drug synthesis. Targeting inflammation in cancer associated with chronic inflammation is a promising therapy. In the present study, we investigated the anti-inflammatory effects of fluorinated benzofuran and dihydrobenzofuran derivatives in macrophages and in the air pouch model of inflammation, as well as their anticancer effects in the human colorectal adenocarcinoma cell line HCT116. Six of the nine compounds suppressed lipopolysaccharide-stimulated inflammation by inhibiting the expression of cyclooxygenase-2 and nitric oxide synthase 2 and decreased the secretion of the tested inflammatory mediators. Their IC₅₀ values ranged from 1.2 to 9.04 μM for interleukin-6; from 1.5 to 19.3 μM for Chemokine (C-C) Ligand 2; from 2.4 to 5.2 μM for nitric oxide; and from 1.1 to 20.5 μM for prostaglandin E₂. Three novel synthesized benzofuran compounds significantly inhibited cyclooxygenase activity. Most of these compounds showed anti-inflammatory effects in the zymosan-induced air pouch model. Because inflammation may lead to tumorigenesis, we tested the effects of these compounds on the proliferation and apoptosis of HCT116. Two compounds with difluorine, bromine, and ester or carboxylic acid groups inhibited the proliferation by approximately 70%. Inhibition of the expression of the antiapoptotic protein Bcl-2 and concentration-dependent cleavage of PARP-1, as well as DNA fragmentation by approximately 80%, were described. Analysis of the structure–activity relationship suggested that the biological effects of benzofuran derivatives are enhanced in the presence of fluorine, bromine, hydroxyl, and/or carboxyl groups. In conclusion, the designed fluorinated benzofuran and dihydrobenzofuran derivatives are efficient anti-inflammatory agents, with a promising anticancer effect and a combinatory treatment in inflammation and tumorigenesis in cancer microenvironments.

Keywords: benzofuran; inflammation; macrophage; HCT116 cells; prostaglandin E₂; cyclooxygenase-2

1. Introduction

Inflammation is the body's immune defense against offending agents that disrupt the integrity of cellular homeostasis, such as infectious agents (bacteria, virus, fungi) or tissue necrosis, to reinstate cellular homeostasis [1]. Failure to repair this disruption causes chronic inflammation that leads, in many cases, to cancer progression [2]. It has been suggested that chronic inflammation participates in tumor initiation (inducing DNA damage and chromosomal abnormalities), promotion (inducing clusters of malignant cells), and progression (inducing angiogenesis and metastasis) [3].

Colorectal cancer (CRC) can be associated with or is raised from chronic inflammation, such as in the case of patients with inflammatory bowel diseases (Crohn's disease or ulcerative colitis) [4]. Inflammatory cytokine and mediator release in the surrounding microenvironment may promote cancer progression and metastasis. Thus, targeting inflammation in CRC patients may be a promising therapeutic approach. Large epidemiological studies have shown that non-steroidal anti-inflammatory drugs (NSAIDs) reduce the risk of CRC and decrease mortality by 30–40% [5]. Evidence was based on the chemoprotective effect of cyclooxygenase-2 (COX-2) selective inhibitors [6]. In addition, COX-2 is highly expressed in CRC and is associated with elevated levels of prostaglandin (PG) E₂ [7]. PGE₂ was shown to activate phosphatidylinositol-4,5-bisphosphate 3-kinase, the PI3K/Akt cell survival pathway. An *in vivo* study has shown that the sequestration of PGE₂ by the administration of PGE₂ monoclonal antibody in mice decreased the growth of the transplantable tumors [8]. Inflammatory mediators such as interleukin (IL)-6 can also mediate tumor proliferation by activating the antiapoptotic protein Bcl-2 [9]. Moreover, inducible nitric oxide (NO) synthase 2 (NOS2) had a significant association with poor survival in human cancer. It may be used as a predictive biomarker for cancer progression [10]. Thus, the combinatory drug that may have anti-inflammatory and anticancer effects could be a promising therapy for tumorigenesis [11].

Benzofuran and dihydrobenzofuran are key pharmacophores that are widespread in many natural products and bioactive compounds. Ailanthoidol, a natural benzofuran, exhibits anticancer, antiviral, immunosuppressive, antioxidant, and antifungal activities [12], whereas eurothiocin B, a representative example of 2,3-dihydrobenzofurans, is an α -glucosidase inhibitor [13]. Griseofulvin and its analogs are known as antiviral and anticancer agents [14,15], and Aurone also has anticancer activity [16]. The importance of fluorine in medicinal chemistry stands, *inter alia*, behind its ability to enhance drug permeability and bioavailability [17]. For this purpose, nine fluorinated benzofuran and dihydrobenzofuran derivatives were synthesized and tested for both anti-inflammatory and anticancer activities. In this present study, the anti-inflammatory effects of these derivatives were assessed by measuring the IL-6, NO, chemokine CCL2, and PGE₂ formation and protein expressions of COX-2 and NOS2 in response to LPS-treated macrophages. In addition, the effects of these derivatives on COX-1 and COX-2 activities were also studied in the presence of arachidonic acid (the COX substrate). For the anticancer effect, HCT116 cells were treated with these derivatives and tested for their ability to inhibit the proliferation and induce apoptosis by testing the Bcl-2 and PARP-1 protein expression, as well as the percentage of DNA cleavage.

2. Results and Discussion

2.1. Effect of Inflammation on Macrophages

We first investigated the capacity of the fluorinated benzofuran and dihydrobenzofuran compounds on inflammation in LPS-treated macrophages. We assessed their inhibitory effects on the release of the proinflammatory mediators PGE₂, IL-6, CCL2, and NO. For the difluorinated compounds of group I (Figure 1), we tested the role of the bromine and carboxyl group. Compounds 2 and 3 were very potent in blocking PGE₂ formation by more than 50% production in response to LPS in macrophages, with IC₅₀ values of 1.92 and 1.48 μ M, respectively (Figure 2A and Table 1). For compounds of group II (Figure 1), which are monofluorinated, both compounds 5 and 6, where R1 is the carboxyl group and the R is a phenyl group and

an isopropyl group, respectively, were very potent inhibitors of PGE₂ production in response to LPS in macrophages (Figure 2A). Finally, compound 8 of group III only showed a partial inhibition of PGE₂ production, with an IC₅₀ of 20.52 μM (Table 1).

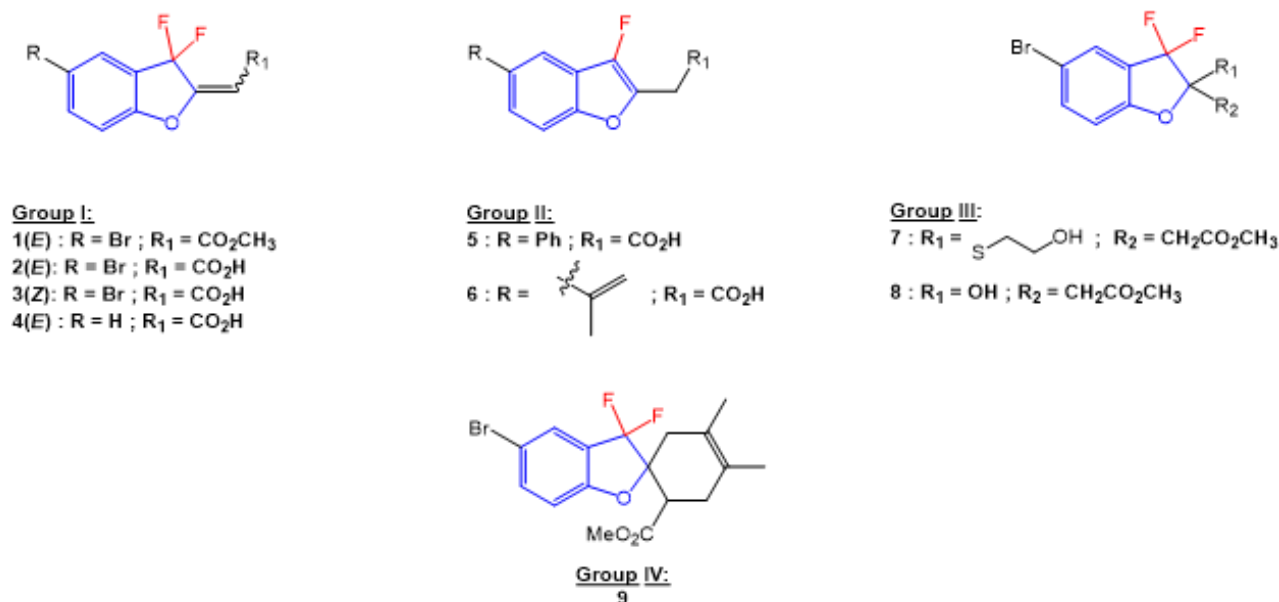


Figure 1. Structures of benzofuran and dihydrobenzofuran derivatives.

Table 1. In vitro effects of compounds 1, 2, 3, 5, 6, and 8 on the release of inflammatory mediators in macrophages.

Compound	IC ₅₀ (μM)			
	PGE ₂	IL-6	CCL2	NO
1	ND	ND	8	ND
2	1.91	1.23	1.52	2.42
3	1.48	5.21	1.5	5.23
5	1.92	ND	ND	ND
6	1.12	ND	ND	ND
8	20.52	9.04	19.27	ND

Next, we evaluated the effect of the benzofuran derivatives on IL-6 and CCL2 in LPS-treated macrophages. Only compounds 2, 3, and 8 significantly decreased the IL-6 production by more than 50% at a concentration of 50 μM, with the IC₅₀ ranging from 1.23 to 9.04 μM (Table 1, Figure 2B). For CCL2, compounds 2, 3, and 8 showed significant decreases (Figure 2C). Compound 1, which was tested at its highest non-toxic concentration (10 μM), showed a moderate effect on CCL2. Compounds 1, 2, and to a lesser extent 3 and 4 were decreased significantly in the mRNA levels of CCL2 and IL-6 in human THP-1-derived macrophages treated with LPS (Figure S3).

In parallel, the effect of the synthesized compounds on the production of NO (Figure 2D) shows that only compounds 2 and 3 were able to significantly decrease NO production, with IC₅₀ values of 2.4 and 5.2 μM, respectively.

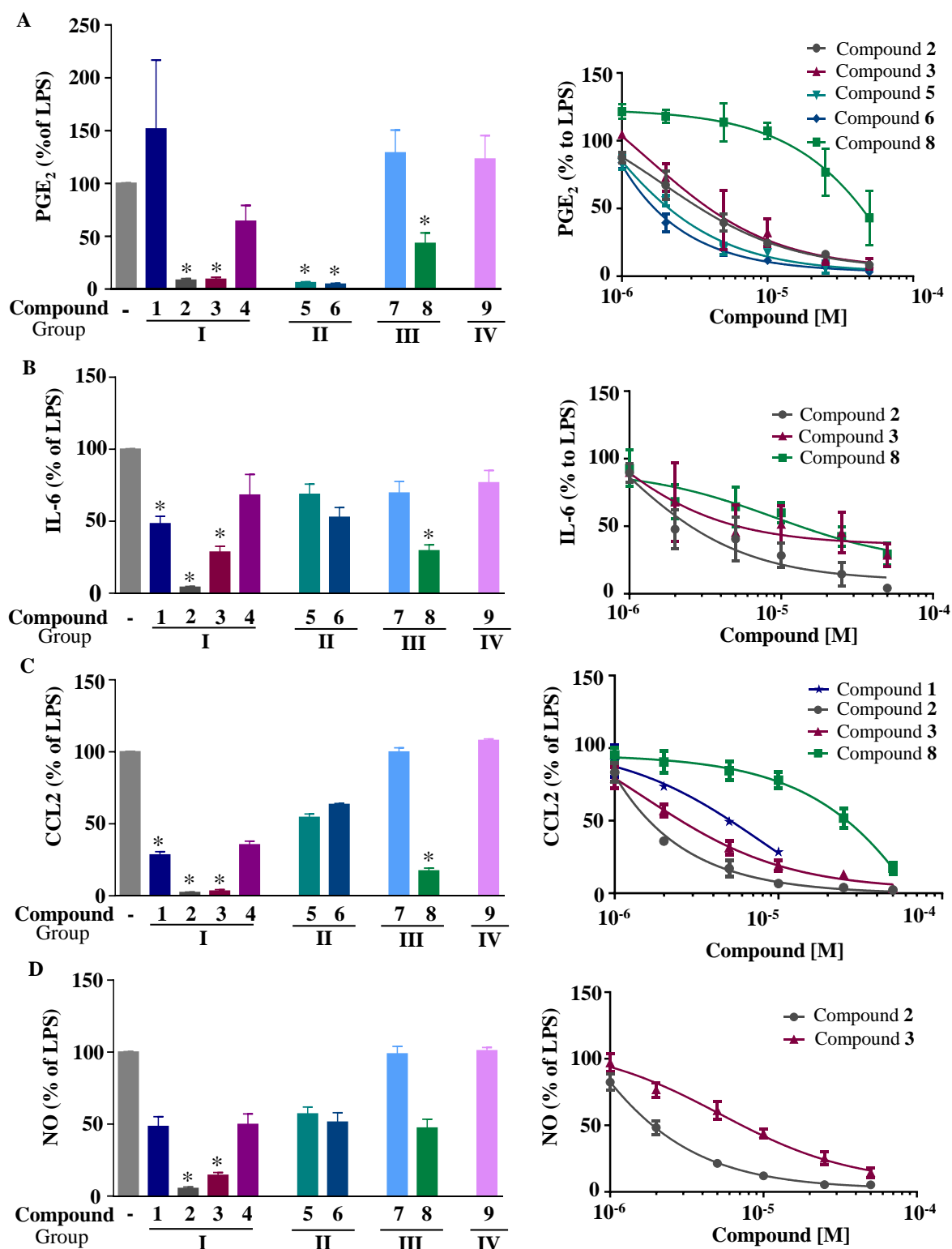


Figure 2. Effects of the fluorinated benzofuran and dihydrobenzofuran on the secretion of PGE₂, IL-6, CCL2, and NO. Macrophages were treated with only 10 μM because of toxicity at higher concentrations for compounds 1, 7, and 9, and 50 μM for the other compounds, prior to the addition of 10 ng/mL LPS for 24 h. The inflammatory mediators measured in the secreted milieu and results were expressed as percentage of LPS, and the corresponding IC₅₀ fitting curves for compounds 2, 3, 5, 6, or 8 using six increasing concentrations were determined. (A) Secreted PGE₂; (B) IL-6; (C) CCL2; and

(D) NO formation. Levels of measured mediators and cytokines were for the basal and LPS-treated macrophages, as follows: PGE₂: 19.9 ± 1.5 and 146 ± 27.2 pg/mL; IL-6: undetermined (for basal) and 19.9 ± 4.3 ng/mL; CCL2: 5.2 ± 0.4 and 54.7 ± 8.1 ng/mL; NO derivatives: 1.3 ± 0.1 μM and 31.4 ± 4.9 μM. Data are represented as mean of percentage of LPS ± SEM of four experiments performed in triplicates; * *p* < 0.05 versus LPS (one-way ANOVA followed by Dunnett's test).

In order to determine whether these compounds have a direct effect on PGE₂ formation, the COX activity and COX-2 expression were assessed. COX-1 activity was determined as the level of PGE₂ synthesized from exogenous added arachidonic acid in HEK-293 cells overexpressing COX-1 (Figure 3A). In a similar setting, we previously showed that ibuprofen, a non-selective COX-1/COX-2 inhibitor, blocked PGE₂ synthesis [18]. COX-2 activity was determined as the concentration of PGE₂ synthesized from exogenous arachidonic acid added on 24 h LPS-treated macrophages, where previous treatment with aspirin was applied to block basal COX (Figure 3C). In this setting, 1 μM NS398, a selective COX-2 inhibitor (Cayman Chemicals, 70590), decreased PGE₂ synthesis by 63% (data not shown). Figure 3B shows that compounds 3 and 6 significantly reduced the COX-1 activity, with IC₅₀ values of 7.9 μM and 5 μM, respectively. In Figure 3D, we can see that compounds 5 and 6 strongly reduced the COX-2 activity, with IC₅₀ values of 28.1 μM and 13 μM, respectively. Compound 3 showed a slight reduction in COX-2 activity. Compounds of group III (Figure 1) were generated from compound 1 and had bromine as the R group, with the ester group as R3, and R2 as the thiol with hydroxyl group for compound 7, and only the hydroxyl group for compound 8. Only compound 8 inhibited partial PGE₂ production in macrophages (Figure 2A) without any effect of COX-1 or COX-2 activities (Figure 3B,D), whereas the replacement of R1 by the thiol-hydroxyl group (compound 7) resulted in the loss of the inhibitory activity (Figures 2A and 3B). Compound 9 did not have any effect (Figures 1A and 3B).

In parallel, we assessed the effects of these compounds on the COX-2 and NOS2 expressions in macrophages. For the COX-2 expression, only compound 2 significantly decreased the COX-2 protein induced by LPS after 24 h of treatment (Figure 4). Replacing the R residue in compound 2 with hydrogen in compound 4 or R1 residue by a methyl ester group in compound 1 resulted in the loss of this inhibitory effect. Compounds 2 and 3 were the only compounds that significantly decreased the NO secretion. Because NO is the breakdown product of NOS2 enzymes, we assessed their effect on the enzyme expression. Figure 4 shows the inhibition of LPS-dependent NOS2 protein expression by compounds 2 and 3. Compounds 1, 2, 3, and 8 did not modify the NF-κB or Iκ-Bα phosphorylation induced by LPS, excluding any effects of the compounds on the NF-κB (Figure S4).

2.2. Effects of Compounds 2, 3, 5, and 6 on Inflammation in Subcutaneous Zymosan-Induced Air Pouch in Mice

The zymosan-injected air pouch model of inflammation has been shown to mimic the synovium cavity and is largely used to assess inhibitors of inflammation [19–22]. To test the anti-inflammatory effects of the synthesized compounds *in vivo*, compounds 2, 3, 5, and 6 were co-administered in the sterile air pouch with zymosan (Figure 5A). At 24 h post-treatment, the number of cells of the air pouch exudates was significantly reduced for compounds 2, 3, 5, and 6, whereas the PGE₂ levels were inhibited by compounds 2, 3, and 6 (Figure 5B). Compounds 2 and 6 inhibited LPS-induced IL-6 production, whereas compounds 3, 5, and 6 inhibited CCL2 formation in response to LPS, as assessed by ELISA (Figure S5). Next, we assessed the effects of these compounds on the gene expressions of several inflammatory biomarkers, including cytokines *Il1a* and *Il1b*, chemokines *Ccl3* and *Ccl4*, and the inflammatory-associated enzymes *Ptgs2* and *Nos2* (Figure 5C), and showed strong inhibition of the proinflammatory genes by compound 2. Compounds 3 and 6 modestly inhibited the expression of *Ccl4*.

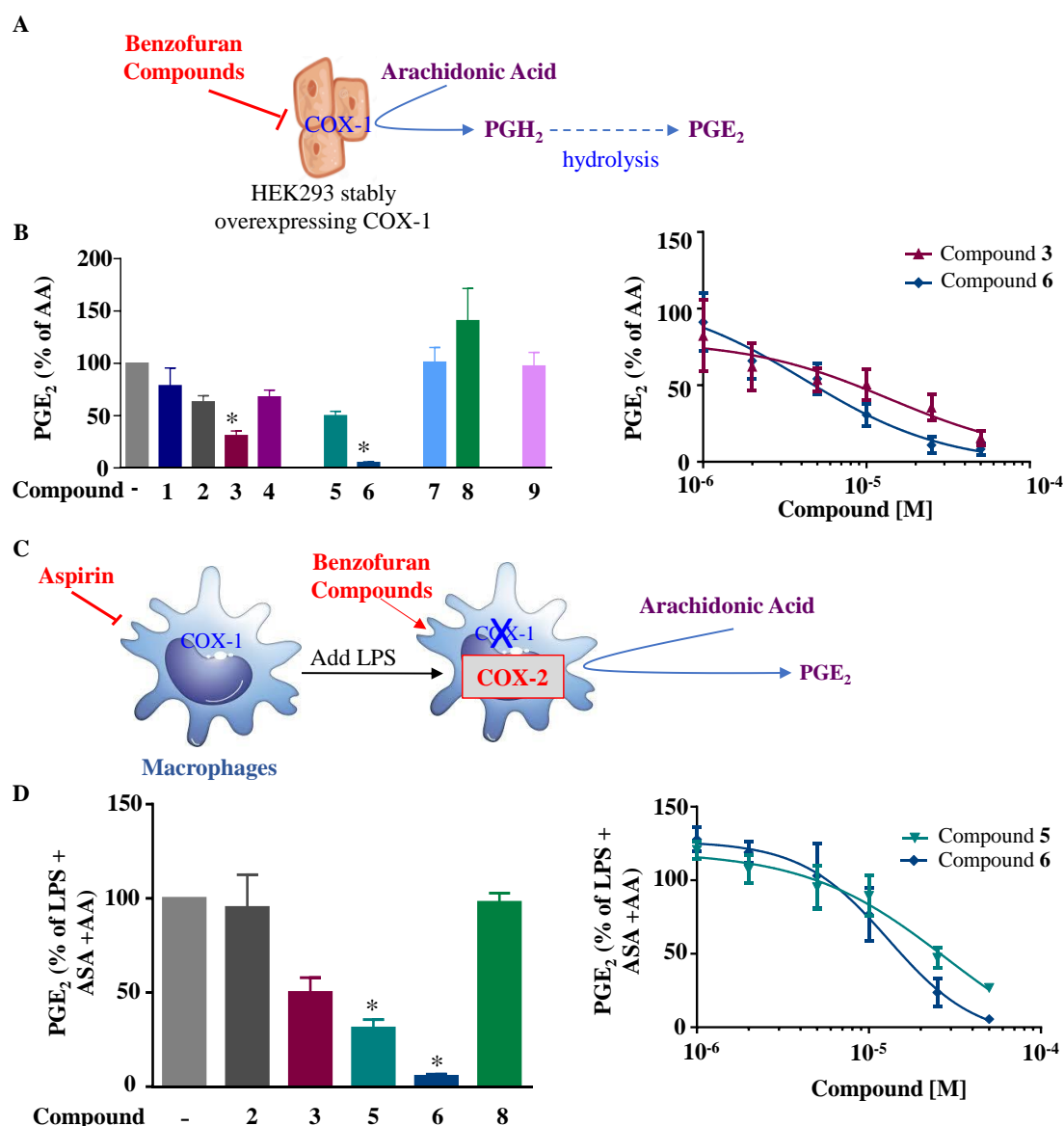


Figure 3. Effects of the fluorinated benzofuran and dihydrobenzofuran on COX-1 and COX-2 activities. (A) Illustration for COX-1 activity assay. HEK-293 cells stably overexpressing COX-1 are treated with the nine derivatives of benzofuran at concentrations of only 10 μ M for compounds 1, 7, and 9, and 50 μ M for the other compounds, 30 min prior to the addition of 10 μ M arachidonic acid (AA). This results in PGE₂ production from PGH₂ after hydrolysis, which reflects the COX-1 activity. (B) COX-1 activity. PGE₂ formation was measured by enzyme immunoassay with the corresponding IC₅₀ fitting curves for compounds 3 and 6. Levels of PGE₂ were very low in the absence of arachidonic acid (0.04 ± 0.01 ng/mL) and 104.3 ± 16.7 ng/mL for 10 μ M AA. (C) Illustration for COX-2 activity determination. Macrophages are treated with 10 μ M of aspirin (ASA) for 30 min to block basal COX activity, washed, and treated with 10 ng/mL LPS for 24 h to induce COX-2. Cells are then washed and incubated 30 min with 50 μ M of the different compounds prior to the addition of 10 μ M of AA. The produced PGE₂ mainly reflects COX-2 activity. (D) COX-2 activity. Percentage of LPS-treated cells was calculated, and data are represented as mean \pm SEM (n = 4); * $p < 0.05$ versus AA for COX-1 activity, and versus LPS + ASA + AA for COX-2 activity (one-way ANOVA followed by Dunnett's test). Corresponding IC₅₀ fitting curves for compounds 5 and 6 are illustrated. Levels of PGE₂ were very low in the absence of arachidonic acid (0.06 ± 0.01 ng/mL) and 71.7 ± 5.7 ng/mL for 10 μ M AA.

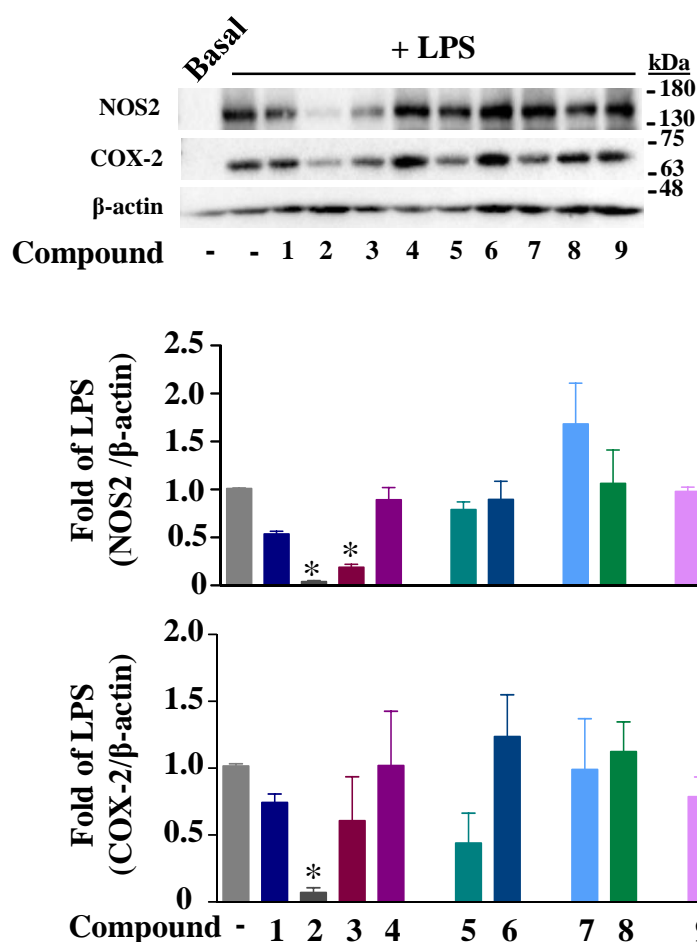


Figure 4. Effects of the fluorinated benzofuran and dihydrobenzofuran on COX-2 and NOS2 protein expressions. COX-2 and NOS2 protein expressions were assessed in macrophages incubated with only 10 μ M for compounds 1, 7, and 9, and 50 μ M for the other compounds, for 30 min prior to the addition of 10 ng/mL LPS for 24 h. β -actin was used as a loading control, and densitometric analysis was performed using ImageJ software (NIH, MA). Data are expressed as fold of LPS-treated macrophages and represented as mean \pm SEM of 4 different experiments; * $p < 0.05$ versus LPS (one-way ANOVA followed by Dunnett's test).

2.3. Anticancer Effect

Because studies have shown that some compounds with anti-inflammatory effects can have anticancerogenic effects, we evaluated the effect of the benzofuran derivatives on cell proliferation and apoptosis. The compounds were tested first for their antiproliferative effect on HCT116 using a WST-1 assay. Cells were treated with 50 and 100 μ M of all the compounds for 72 h. Figure 6A shows that only compounds 1 and 2 inhibited cell proliferation by more than 50%, with IC_{50} values of 19.5 and 24.8 μ M, respectively. A TUNEL assay was performed to assess the effect of these two compounds on apoptosis [23]. HCT116 cells were treated with compounds 1 and 2 at increasing concentrations (10, 25, and 50 μ M) for 72 h. Figure 6B shows the concentration-dependent increase in the percentage of apoptotic cells for compounds 1 and 2. Furthermore, the expression of the antiapoptotic protein Bcl-2 [24] was decreased by compounds 1 and 2 in a concentration-dependent manner in parallel to the increase in the protein level of cleaved PARP-1, a marker of apoptosis [25] (Figure 6C).

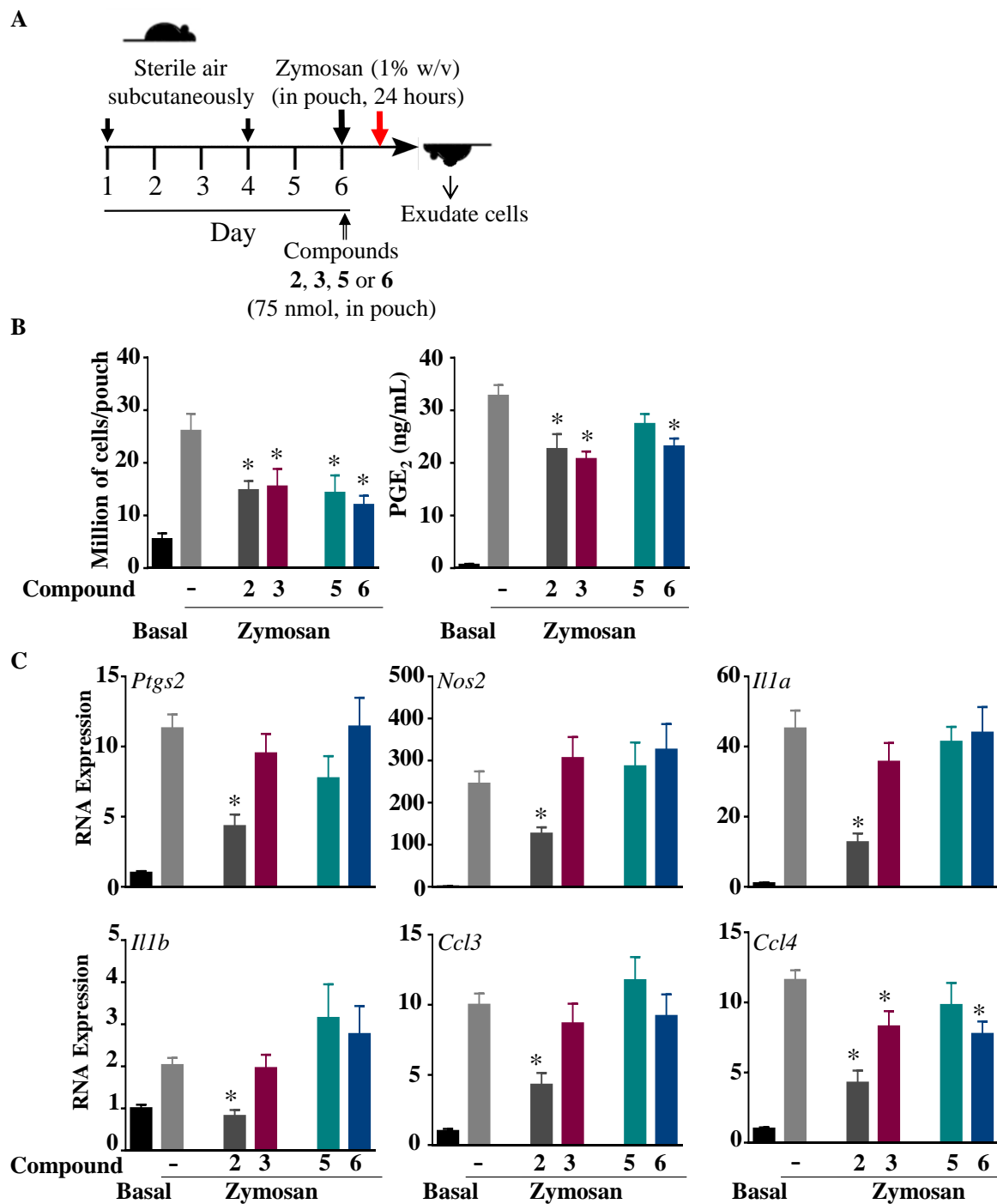


Figure 5. Effect of fluorinated benzofuran and dihydrobenzofuran on inflammation in the zymosan-treated sterile air pouch model in mice. (A) A timeline for the zymosan-induced inflammation experiments of the air pouch model in C57/BL6 mice. The pouch was formed on day 1 and refilled on day 4 with sterile air. Mice were injected at day 6 with 1% zymosan (*w/v* in saline), or 0.5 mL of saline for control mice. An amount of 50 nmol of compounds 2, 3, 5, and 6, or vehicle, were co-injected into the air pouch. At 24 h post-treatment, exudates were collected. (B) Recruited cells in the pouch and PGE₂ production. (C) Gene expressions of inflammatory enzymes *Ptgs2* and *Nos2*, proinflammatory cytokines *Il1a* and *Il1b*, and chemokines *Ccl3* and *Ccl4*. Data correspond to the mean ± SEM (n = 6–8 mice per group); * *p* < 0.05 compared to the zymosan-treated cells (one-way ANOVA followed by Dunnett's test).

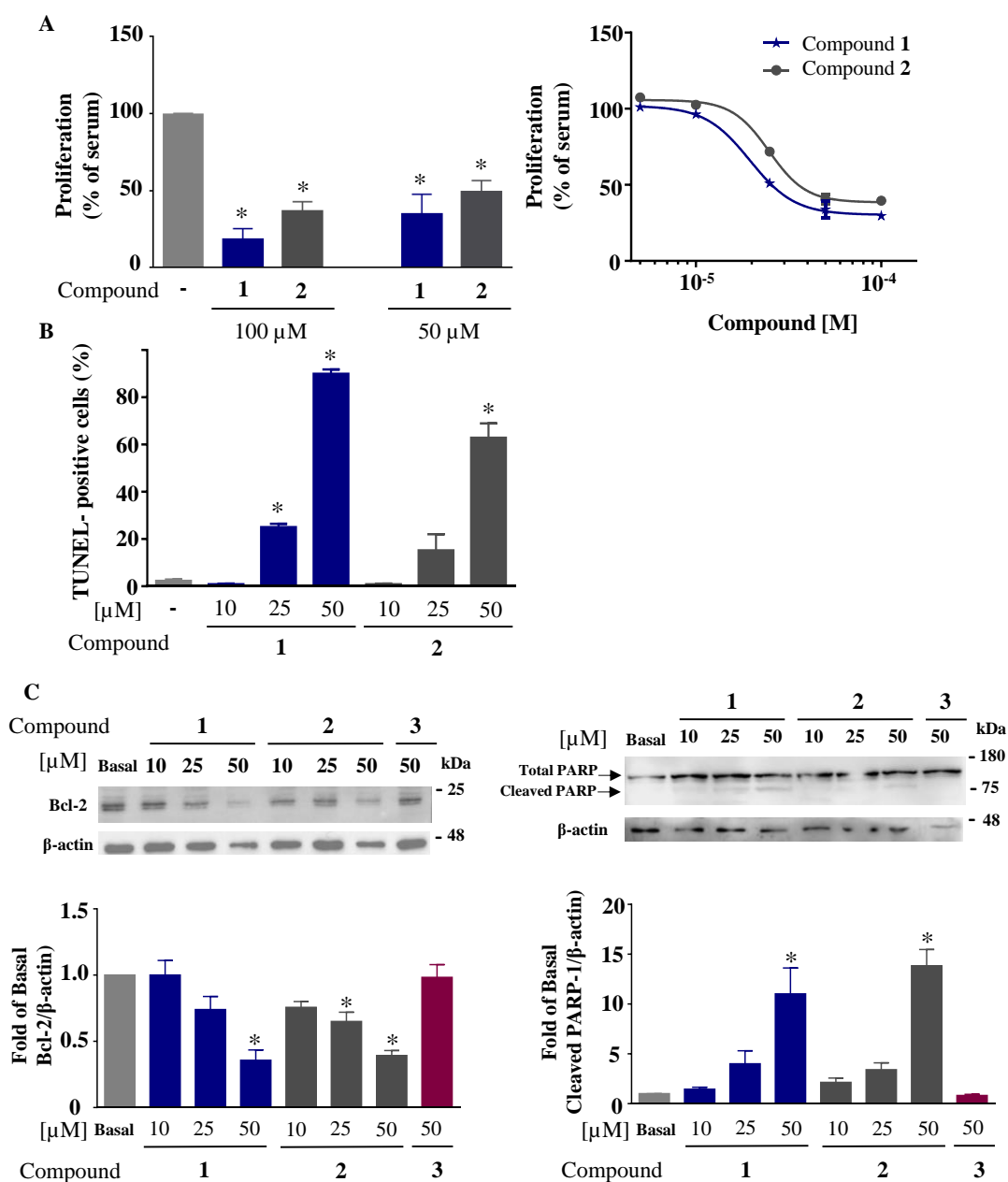


Figure 6. Effect of dihydrofluorinated benzofuran derivatives on HCT116 proliferation, DNA cleavage, PARP-1 cleavage, and Bcl-2 expression. **(A)** For proliferation, HCT116 cells were treated with 50 and 100 μ M of all compounds for 72 h, and the percentage of viable cells was measured by WST-1 assay. The corresponding IC_{50} fitting curves for only the positive compounds **1** and **2**. **(B)** TUNEL assay for detecting the percentage of apoptotic cells (cleaved DNA) after treating with compounds **1** and **2** at 10, 25, and 50 μ M for 72 h, compared to vehicle-treated cells showing no DNA cleavage (no treatment). **(C)** Western blot for Bcl-2 and cleaved PARP-1 after treatment of cells with compounds **1** and **2** at concentrations of 10, 25, and 50 μ M for 72 h. Compound **3** was used as a negative control. β -actin was used as loading control. Data are represented as percentage mean \pm SEM ($n = 3$); * $p < 0.05$ versus vehicle-treated cells (basal) (one-way ANOVA followed by Dunnett's test).

3. Materials and Methods

3.1. Materials

Arachidonic acid (90010), LPS (serotype 0111:B4, 19661), and PGE₂-tracer (400140) for the PGE₂ measurement were from Cayman Chemicals Co. (Ann Arbor, MI, USA), and ELISA kits for IL-6 and RT-PCR reagents were from Thermo Fisher Scientific (Waltham, MA, USA). All

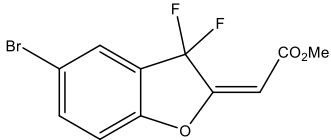
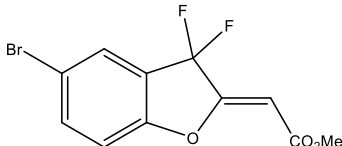
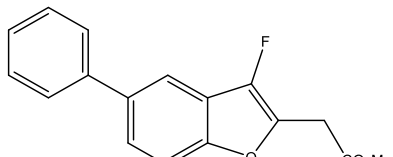
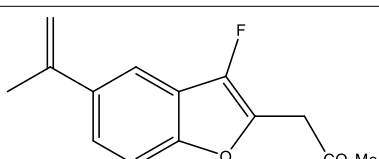
chemicals for the synthesis of the benzofuran derivatives, cell culture media and the WST-1 kit were from Sigma Aldrich (St. Louis, MO, USA), and all those for electrophoresis, protein quantification, and Western blot were from Bio-Rad Laboratories (Hercules, CA, USA).

3.2. Synthesis of Fluorinated Benzofuran

Nine derivatives of benzofuran and dihydrobenzofuran with different structures were studied in this work (Figure 1).

The synthesis of compounds **1**, **7**, **8**, and **9** was described in our previous work [26]. Five novel derivatives, **2**, **3**, **4**, **5**, and **6**, were prepared by saponification of the corresponding esters (LiOH in THF/H₂O and then acidification), purified by chromatography, and isolated with good yields (Table 2). NMR for the newly synthesized molecules is presented in the Supplementary Materials.

Table 2. Synthesis and yield of carboxylic acids **2**, **3**, **4**, **5**, and **6**.

Compound	Starting Compound	Yield
2		63%
3		70%
4		78%
5		68%
6		71%

3.3. Evaluation of Inflammation in Bone Marrow-Derived Macrophages (BMDMs)

C57BL/6J (10–15 weeks old) male mice were obtained from the animal care facility at the American University of Beirut. All animal procedures were performed following the recommendations of the IACUC (Institutional Animal Care and Use Committee approval 16-09-M379). BMDMs were prepared and characterized as described previously by our group [27]. BMDMs were isolated from C57BL/6J mice by flushing the femur and tibia with RPMI-1640 culture media (Sigma-Aldrich R7388), and cells were collected and centrifuged at 300× g for 5 min. The supernatant was discarded, and the pellet was resuspended in 2 mL red blood lysis 10% (Sigma-Aldrich R7767) medium in PBS and incubated for 5 min at room temperature. After diluting the suspension of cells with 5 mL of RPMI containing 10% FBS and 1% penicillin–streptomycin, cells were centrifuged at 300× g for 5 min, and the

cell pellet was resuspended in RPMI media containing 10% FBS supplemented with 15% L929-conditioned medium containing macrophage-colony stimulating factor (M-CSF1) and plated on 100 Petri dishes. Cells were allowed to proliferate and differentiate for 5–6 days. Cells were harvested, washed, and allowed to adhere overnight in RPMI containing 10% FBS for treatment. Cells were previously characterized by flow cytometry as macrophages using this method [28]. We used male C57BL/6J mice, as comparable responses to LPS were seen when using male or occasionally female mice (IL-6 levels varied from 4 to 20 ng/mL and from 6 to 20 ng/mL for female and male mice, respectively, and CCL2 levels varied from 1.5 to 5 ng/mL and from 2.1 to 7 ng/mL for female and male mice, respectively). Cells were plated at 0.8×10^6 cells per 3.8 cm² well [27].

3.4. Cell Treatment

BMDMs were then treated with different concentrations of the benzofuran and dihydrobenzofuran derivatives for 30 min prior to the addition of 10 ng/mL LPS for 24 h. Vehicle (dimethyl sulfoxide, DMSO) concentration did not exceed 0.4% and had no effect. The supernatants were assessed for IL-6, PGE₂, CCL2, and nitrite, the stable derivative of NO, as described previously [19,28].

3.5. Cyclooxygenase Activity

COX-1 and COX-2 activities were performed as described previously [28] in human embryonic kidney cell line (HEK-293) stably overexpressing COX-1 [19] and in macrophages, respectively. Macrophages were first treated for 30 min with 10 μM acetylsalicylic acid (ASA) (Sigma-Aldrich, A5376) to irreversibly inhibit COXs and washed twice with PBS, prior to the addition of LPS for 24 h to induce COX-2. For both COX-1 and COX-2 assays, the benzofuran compounds were then added to the cells for 30 min prior to the incubation with 10 μM arachidonic acid for another 30 min. PGE₂ was then measured using an enzyme immunoassay, as described previously [19,28].

3.6. Subcutaneous Dorsal Air Pouch Model

C57BL/6J female mice (8-week-old, 20–25 g) were kept at 5 per cage on a 12 h light–dark cycle with cotton cocoon as enrichment in temperature- and humidity-controlled rooms. Mice were provided with food and water *ad libitum*, and food intake and body weight were monitored throughout the study period. Approval for use of animals was obtained from the IACUC (16-11-393). Dorsal air pouches were created in mice as previously described [19,28]. Six days after the initial injection of sterile air, 0.5 mL of saline containing 100 μM of benzofuran compounds **2**, **3**, **5**, or **6** (50 nmol per pouch) or 0.2% DMSO as vehicle was co-injected in the pouch with 0.5 mL of 0.9% saline (for the control group) or 0.5 mL of 1% zymosan (*w/v*, for zymosan and zymosan + compound) (Sigma-Aldrich, 400140). At 24 h after treatment, the animals were sacrificed by CO₂ inhalation and the air pouch washed, the exudates collected, and the cell number determined. As previously reported, the main subtype of leukocytes present in the air pouch were neutrophils (75%) and monocytes–macrophages (12–15%), as determined by selective flow cytometry [20]. The concentrations of PGE₂, CCL2, and IL-6 and the gene expression were assessed as described previously [19,20,28].

3.7. Reverse Transcriptase-PCR (RT-PCR)

For gene expression, RT-PCR was performed as described previously [20]. Briefly, cell pellets obtained by centrifugation of air pouch exudates at $300 \times g$ for 5 min at 4 °C were suspended in TriPure (Sigma Aldrich 11667165001). An amount of 2 μg of total RNA was reverse-transcribed using iScript cDNA synthesis kit (Bio-Rad Laboratories, 1708891). RT-PCR was carried out on CFX384 cyler using iTaq Universal SYBR Green Supermix kit (Bio-Rad Laboratories, 1725121) and the primers obtained from TIB Molbiol (Berlin, Germany). Oligonucleotide sequences were according to the references [29–31], except for *Ptgs2* and *Nos2*, which were as follows: *Ptgs2* (F): AGACAGATTGCTGGCCGGGTTGCT;

Ptgs2 (R): TCAATGGAGGCCTTTGCCACTGCT; *Nos2* (F): CCCTTGCTGCTGTTCTCAGC-CCAAC; *Nos2* (R): GGACGGGTCGATGTCACATGCA. Gene expression was calculated using $\Delta\Delta CT$ method relative to the housekeeping gene 18S.

3.8. Toxicity Assay

WST-1 assay (Sigma-Aldrich, 5015944001) was used to determine the toxicity of the synthesized compounds on BMDM and HCT116 (ATCC, CCL-247), kindly provided by Dr. Nadine Darwiche, Department of Biochemistry and Molecular Genetics, American University of Beirut, Lebanon. Briefly, macrophages (50,000 cells per well) and HCT116 (20,000 cells per well) were plated in a 96-well plate in RPMI 1640 culture medium containing 10% fetal bovine serum (FBS) and grown for 24 h. Cells (in triplicates) were treated with 10 or 50 μM of the compounds for macrophages, and 50 or 100 μM for HCT116. Culture medium without cells and cells without treatment were used as basal and maximal activity, respectively. Results were expressed as percentage of cells without treatment. For macrophages, all compounds showed 95% viability at both concentrations except for compounds **1**, **7**, and **9**, with only 50% viability at 50 μM , which were further used at 10 μM (Figure S1). However, all compounds showed 95% viability at 100 μM in HCT116 (Figure S2).

3.9. Proliferation Assay

WST-1 assay was used to determine the effect of these compounds on HCT116 proliferation. Cells were plated in 96-well plate in triplicates (5000 cells per well) for 24 h and treated with 50 and 100 μM of the different compounds for 72 h. For compounds that exhibited strong antiproliferative effects, a dose-response curve was conducted with 5 concentrations (5, 10, 20, 50, and 100 μM). Culture medium without or with 10% FBS alone was used as basal and maximal proliferation, respectively. Results were expressed as percentage of cells incubated with 10% FBS alone.

3.10. Western Blot

Macrophages were incubated with the compounds for 30 min prior to the addition of 10 ng/mL LPS for 24 h. Protein levels for COX-2 and NOS2 were detected in LPS-stimulated macrophages. As previously described [28], 10 μg of total protein was assessed. The primary antibodies were developed and characterized as previously described: for COX-2, mouse monoclonal antibody anti-COX-2 (clone COX-214, 1/5000) [32]; for NOS2, rabbit polyclonal antibody anti-NOS2 (dilution 1/2000 [33]). Antibodies anti-phospho-NF- κB (3033S), phospho-I $\kappa\text{B}\alpha$ (9246S), and total I $\kappa\text{B}\alpha$ (4814S) were from Cell Signaling Technologies (Danvers, MA, USA). Total NF- κB C-20 (sc-372) was from Santa Cruz Biotechnologies (Dallas, TX, USA), and mouse β -actin (dilution 1/10,000) (Sigma-Aldrich, A5441). Clarity™ western ECL substrate (Bio-Rad Laboratories 10-5061) was used according to the manufacturer's instructions to reveal positive bands visualized using Bio-Rad ChemiDoc. For Bcl-2 and cleaved PARP-1, HCT116 cells were plated in 6-well plates (200,000 cells per well) for 24 h, and treated with compounds **1** and **2** at 10, 25, and 50 μM for 72 h. Supernatants and cells were collected and lysed using RIPA lysis buffer containing inhibitors of protease. Western blot of Bcl-2 and cleaved PARP-1 was performed using 25 μg of total protein with a rabbit polyclonal antibody anti-Bcl-2 (1/500) (Santa Cruz Biotechnology, sc-492), rabbit polyclonal antibody anti-PARP-1 (1/1000) (Santa Cruz Biotechnology, sc-7150), and mouse anti- β -actin (dilution 1/10,000) (Sigma-Aldrich, A5441).

3.11. TUNEL Assay

Terminal deoxynucleotidyl transferase dUTP nick-end labeling (TUNEL) assay (Sigma Aldrich 11684795910) was conducted to detect late phase of apoptosis in HCT116 cells. Cells were plated in 6-well plate (200,000 cells per well) for 24 h, and treated with compounds **1** and **2** at 10, 25, and 50 μM for 72 h. Adherent cells and cells in supernatants were collected and fixed with 4% paraformaldehyde for 2 days and then treated with PBS containing 0.1% Triton X-100 at 4 °C for 2 min. Cells were then stained with the TUNEL reagent for 1 h,

and positive signals were quantified using the Guava EasyCyte8 Flow Cytometer-Millipore according to the manufacturer's instructions.

3.12. Data Analysis

IL-6, CCL2, nitrite (for NO), and PGE₂ concentrations from 3–5 independent experiments were expressed as percentage of LPS alone and as mean \pm SEM. COX activity was determined as percentage of PGE₂ produced from exogenous arachidonic acid. Curve fitting and calculation of IC₅₀ values were performed using GraphPad Prism (version 9.5.1 Software, La Jolla, CA, USA).

Densitometric analyses were performed using ImageJ software (NIH, MA, USA). The ratio of the different analyzed bands to β -actin was determined and data are represented as fold change compared to the LPS-treated cells. Percentage of viable cells for proliferation assay was determined as percentage to control (non-treated cells). For TUNEL assay, apoptotic cells were quantified, and results were expressed as percentage to positive cells (cleaved DNA) compared to control (non-treated cells). Statistical analysis was performed using one-way ANOVA, followed by Dunnett's multiple comparisons test using GraphPad Prism software. Differences were considered significant when $p < 0.05$.

4. Conclusions

Benzofuran derivatives were shown to have important pharmacological activities, including anticancer, antibacterial, antifungal, analgesic, and many others [34]. Adding fluorine molecules to benzofuran can enhance its bioavailability and permeability [35]. For this, we used nine newly synthesized dihydrofluorinated benzofuran derivatives and aimed to find out which compounds have a dual effect: anti-inflammatory and anticancer, with a potential application in the types of cancer associated with chronic inflammation, such as CRC. The reason behind this is the link between inflammatory mediators and cancer progression. For example, it was found that IL-6 promotes tumor progression by activating the MAPK pathway, which is known to induce tumor proliferation [16]. Others have shown that the chemokine CCL2 induces tumor proliferation and migration by activating the Akt pathway and matrix metalloproteases [36]. For COX-2, several studies have shown its implication in CRC progression, as its protein expression was significantly increased, especially in the latest stages of cancer. The inhibition of COX-2 expression or activity was also demonstrated to lower tumor progression in vivo [37]. One of the mechanisms might be the decrease in Bcl-2 expression, as it was shown that PGE₂ can activate Bcl-2 expression; thus, by inhibiting COX-2, PGE₂ is decreased, and thus Bcl-2 will also decrease, leading to tumor regression [38].

All these findings prompt us to synthesize combinatory molecules working on inhibiting inflammatory mediators, as well as on targeting cancer progression and inducing apoptosis. In our study, six out of nine compounds showed important anti-inflammatory effects with different efficiencies (1, 2, 3, 5, 6, and 8) on PGE₂, IL-6, CCL2, NO, and COX-1/2 activities, and on the COX-2 and NOS2 expressions. Among these six molecules, two were shown to have important anticancer effects (1 and 2) by inhibiting HCT116 proliferation, inducing PARP-1 and DNA cleavages, in parallel with a decrease in Bcl-2 expression. These compounds are difluorinated, having bromine as the R group, and with either formic acid (carboxylic acid group) for compound 1 or ethanoate (ester group) for compound 2 for the R1 group. Compounds 1, 2, 3, and 8 have bromine as the R group and different groups at R1 and R2, which may support the difference in the efficiency of each molecule. Compound 4, which lacks any of the biological effects tested, has a similar structure to compound 2 except for the bromine; thus, for benzofuran derivatives, bromine is important for the anti-inflammatory effect. Compounds 7 and 9 shared the same structure as compounds 1, 2, 3, and 8, but with differences in the R1 and R2, which were bulky and may stand behind their negative effects. Finally, compounds 5 and 6, monofluorinated benzofuran derivatives with R groups other than bromine, such as in compounds 3 and 2, showed a direct inhibitory effect on both COX-1 and COX-2 activities and no effect of COX-2 or

NOS2 expression. This suggests that monofluorination is necessary for the inhibition of COX activities.

Overall, all these results showed the importance of some structural groups of benzofuran, mainly bromine and fluorine, on anti-inflammatory and antiproliferative effects. In the present exploratory study, we identified some novel benzofuran molecules with the desired dual biological action (i.e., anti-inflammatory and anticancer). Compounds **1** and **2** are promising. In the near future, we aim to improve such properties and, based on molecular modeling studies, use these compounds in order to design improved analogues to be synthesized.

Supplementary Materials: The following supporting information can be downloaded at <https://www.mdpi.com/article/10.3390/ijms241210399/s1>.

Author Contributions: Conceptualization, S.E.G., R.G., A.H. (Ali Hachem), E.H. and A.H. (Aida Habib); formal analysis, A.J.A. and A.H. (Aida Habib); funding acquisition, S.E.G., A.H. (Ali Hachem), E.H. and A.H. (Aida Habib); investigation, A.J.A., G.A.E.-A., L.M.A., L.H., R.H.H. and Z.I.M.; methodology, A.J.A., L.H., R.G. and A.H. (Ali Hachem); project administration, S.E.G., A.H. (Ali Hachem), E.H. and A.H. (Aida Habib); resources, B.B., A.H. (Ali Hachem), E.H. and A.H. (Aida Habib); supervision, S.E.G., A.H. (Ali Hachem), E.H. and A.H. (Aida Habib); validation, A.J.A., G.A.E.-A., L.H., R.H.H., L.M.A. and Z.I.M.; writing—original draft, A.J.A. and A.H. (Aida Habib); writing—review and editing, A.J.A., G.A.E.-A., S.E.G., L.H., R.H.H., L.M.A., Z.I.M., B.B., R.G., A.H. (Ali Hachem), E.H. and A.H. (Aida Habib). All authors have read and agreed to the published version of the manuscript.

Funding: This work was supported by the Research Grant Program at the Lebanese University, Lebanon, fund number 21143 (Ali Hachem, Sandra Ghayad, and Eva Hamade). Open-access funding was provided by the College of Medicine, QU Health, Qatar University.

Institutional Review Board Statement: The animal study protocol was approved by the Institutional Review Board (or Ethics Committee) of the American University of Beirut, Institutional Animal Care and Use Committee (IACUC), approval # 16-09-M379 for the BMDM and IACUC approval # 16-11-393 for the air pouch model of inflammation.

Informed Consent Statement: Not applicable.

Data Availability Statement: The data used to support the findings of this study are available from the corresponding author upon request.

Acknowledgments: We thank the Centre Régional de Mesures Physiques de l'Ouest (CRMPO) in Rennes, France, for the mass spectral analysis. We thank all members of the teams (Beirut and Rennes) for their kind help and stimulating discussions.

Conflicts of Interest: The authors declare that they have no competing interests.

Abbreviations

AA: arachidonic acid; ASA: acetylsalicylic acid; Bcl-2: B-cell lymphoma 2; BMDMs: bone marrow-derived macrophages; CCL2: C-C Motif Chemokine Ligand 2; COX: cyclooxygenase; CRC: colorectal cancer; FBS: fetal bovine serum; IL-6: interleukin-6; LPS: lipopolysaccharide; MAPK: mitogen-activated protein kinase; NO: nitric oxide; NOS2: nitric oxide synthase 2; NSAIDs: non-steroidal anti-inflammatory drugs; PARP-1: Poly (ADP-Ribose) Polymerase 1; PGE₂: prostaglandin E₂; TUNEL: terminal deoxynucleotidyl transferase dUTP nick-end labeling.

References

1. Rankin, L.C.; Artis, D. Beyond Host Defense: Emerging Functions of the Immune System in Regulating Complex Tissue Physiology. *Cell* **2018**, *173*, 554–567. [[CrossRef](#)]
2. Chen, L.; Deng, H.; Cui, H.; Fang, J.; Zuo, Z.; Deng, J.; Li, Y.; Wang, X.; Zhao, L. Inflammatory responses and inflammation-associated diseases in organs. *Oncotarget* **2018**, *9*, 7204–7218. [[CrossRef](#)] [[PubMed](#)]
3. Korniluk, A.; Koper, O.; Kemon, H.; Dymicka-Piekarska, V. From inflammation to cancer. *Ir. J. Med. Sci.* **2017**, *186*, 57–62. [[CrossRef](#)] [[PubMed](#)]

4. Izano, M.; Wei, E.K.; Tai, C.; Swede, H.; Gregorich, S.; Harris, T.B.; Klepin, H.; Satterfield, S.; Murphy, R.; Newman, A.B.; et al. Chronic inflammation and risk of colorectal and other obesity-related cancers: The health, aging and body composition study. *Int. J. Cancer* **2016**, *138*, 1118–1128. [[CrossRef](#)] [[PubMed](#)]
5. Hamoya, T.; Fujii, G.; Miyamoto, S.; Takahashi, M.; Totsuka, Y.; Wakabayashi, K.; Toshima, J.; Mutoh, M. Effects of NSAIDs on the risk factors of colorectal cancer: A mini review. *Genes Environ.* **2016**, *38*, 6. [[CrossRef](#)]
6. Patrignani, P.; Patrono, C. Aspirin and Cancer. *J. Am. Coll. Cardiol.* **2016**, *68*, 967–976. [[CrossRef](#)]
7. Wang, D.; Dubois, R.N. The role of COX-2 in intestinal inflammation and colorectal cancer. *Oncogene* **2010**, *29*, 781–788. [[CrossRef](#)]
8. Greenhough, A.; Smartt, H.J.; Moore, A.E.; Roberts, H.R.; Williams, A.C.; Paraskeva, C.; Kaidi, A. The COX-2/PGE2 pathway: Key roles in the hallmarks of cancer and adaptation to the tumour microenvironment. *Carcinogenesis* **2009**, *30*, 377–386. [[CrossRef](#)]
9. Vainer, N.; Dehlendorff, C.; Johansen, J.S. Systematic literature review of IL-6 as a biomarker or treatment target in patients with gastric, bile duct, pancreatic and colorectal cancer. *Oncotarget* **2018**, *9*, 29820–29841. [[CrossRef](#)]
10. Liao, W.; Ye, T.; Liu, H. Prognostic Value of Inducible Nitric Oxide Synthase (iNOS) in Human Cancer: A Systematic Review and Meta-Analysis. *BioMed Res. Int.* **2019**, *2019*, 6304851. [[CrossRef](#)]
11. Napiorkowska, M.; Cieslak, M.; Kazmierczak-Baranska, J.; Krolewska-Golinska, K.; Nawrot, B. Synthesis of New Derivatives of Benzofuran as Potential Anticancer Agents. *Molecules* **2019**, *24*, 1529. [[CrossRef](#)]
12. Kao, C.; Chen, J. A convenient synthesis of naturally occurring benzofuran ailanthoidol. *Tetrahedron* **2001**, *42*, 1111–1113. [[CrossRef](#)]
13. Liu, Z.; Xia, G.; Chen, S.; Liu, Y.; Li, H.; She, Z. Eurothiocin A and B, sulfur-containing benzofurans from a soft coral-derived fungus *Eurotium rubrum* SH-823. *Mar. Drugs* **2014**, *12*, 3669–3680. [[CrossRef](#)]
14. Singh, P.; Rathinasamy, K.; Mohan, R.; Panda, D. Microtubule assembly dynamics: An attractive target for anticancer drugs. *IUBMB Life* **2008**, *60*, 368–375. [[CrossRef](#)]
15. Ho, Y.S.; Duh, J.S.; Jeng, J.H.; Wang, Y.J.; Liang, Y.C.; Lin, C.H.; Tseng, C.J.; Yu, C.F.; Chen, R.J.; Lin, J.K. Griseofulvin potentiates antitumorigenesis effects of nocodazole through induction of apoptosis and G2/M cell cycle arrest in human colorectal cancer cells. *Int. J. Cancer* **2001**, *91*, 393–401. [[CrossRef](#)]
16. Costa-Pereira, A.P. Regulation of IL-6-type cytokine responses by MAPKs. *Biochem. Soc. Trans.* **2014**, *42*, 59–62. [[CrossRef](#)]
17. Purser, S.; Moore, P.R.; Swallow, S.; Gouverneur, V. Fluorine in medicinal chemistry. *Chem. Soc. Rev.* **2008**, *37*, 320–330. [[CrossRef](#)] [[PubMed](#)]
18. Hirz, T.; Khalaf, A.; El-Hachem, N.; Mrad, M.F.; Abdallah, H.; Creminon, C.; Gree, R.; Merhi, R.A.; Habib, A.; Hachem, A.; et al. New analogues of 13-hydroxyocatdecadienoic acid and 12-hydroxyeicosatetraenoic acid block human blood platelet aggregation and cyclooxygenase-1 activity. *Chem. Central J.* **2012**, *6*, 152. [[CrossRef](#)] [[PubMed](#)]
19. El-Achkar, G.A.; Jouni, M.; Mrad, M.F.; Hirz, T.; El Hachem, N.; Khalaf, A.; Hammoud, S.; Fayyad-Kazan, H.; Eid, A.A.; Badran, B.; et al. Thiazole derivatives as inhibitors of cyclooxygenases in vitro and in vivo. *Eur. J. Pharmacol.* **2015**, *750*, 66–73. [[CrossRef](#)] [[PubMed](#)]
20. El-Achkar, G.A.; Mrad, M.F.; Mouawad, C.A.; Badran, B.; Jaffa, A.A.; Motterlini, R.; Hamade, E.; Habib, A. Heme oxygenase-1-Dependent anti-inflammatory effects of atorvastatin in zymosan-injected subcutaneous air pouch in mice. *PLoS ONE* **2019**, *14*, e0216405. [[CrossRef](#)] [[PubMed](#)]
21. Posadas, I.; Terencio, M.C.; Guillen, I.; Ferrandiz, M.L.; Coloma, J.; Paya, M.; Alcaraz, M.J. Co-regulation between cyclo-oxygenase-2 and inducible nitric oxide synthase expression in the time-course of murine inflammation. *Naunyn Schmiedebergs Arch. Pharmacol.* **2000**, *361*, 98–106. [[CrossRef](#)]
22. Vicente, A.M.; Guillen, M.I.; Habib, A.; Alcaraz, M.J. Beneficial effects of heme oxygenase-1 up-regulation in the development of experimental inflammation induced by zymosan. *J. Pharmacol. Exp. Ther.* **2003**, *307*, 1030–1037. [[CrossRef](#)]
23. Plesca, D.; Mazumder, S.; Almasan, A. DNA damage response and apoptosis. *Methods Enzymol.* **2008**, *446*, 107–122. [[CrossRef](#)]
24. Edlich, F. BCL-2 proteins and apoptosis: Recent insights and unknowns. *Biochem. Biophys. Res. Commun.* **2018**, *500*, 26–34. [[CrossRef](#)]
25. Chaitanya, G.V.; Steven, A.J.; Babu, P.P. PARP-1 cleavage fragments: Signatures of cell-death proteases in neurodegeneration. *Cell Commun. Signal.* **2010**, *8*, 31. [[CrossRef](#)]
26. Hariss, L.; Bouhadir, K.; Roisnel, T.; Grée, R.; Hachem, A. Synthesis of Novel Fluorinated Benzofurans and Dihydrobenzofurans. *Synlett* **2017**, *28*, 195–200. [[CrossRef](#)]
27. Habib, A.; Chokr, D.; Wan, J.; Hegde, P.; Mabire, M.; Siebert, M.; Ribeiro-Parenti, L.; Le Gall, M.; Lettéron, P.; Pilard, N.; et al. Inhibition of monoacylglycerol lipase, an anti-inflammatory and antifibrogenic strategy in the liver. *Gut* **2018**, *68*, 522–532. [[CrossRef](#)] [[PubMed](#)]
28. Ayoub, A.J.; Hariss, L.; El-Hachem, N.; El-Achkar, G.A.; Ghayad, S.E.; Dagher, O.K.; Borghol, N.; Gree, R.; Badran, B.; Hachem, A.; et al. gem-Difluorobisaryllic derivatives: Design, synthesis and anti-inflammatory effect. *BMC Chem.* **2019**, *13*, 124. [[CrossRef](#)] [[PubMed](#)]
29. Lodder, J.; Denaes, T.; Chobert, M.N.; Wan, J.; El-Benna, J.; Pawlotsky, J.M.; Lotersztajn, S.; Teixeira-Clerc, F. Macrophage autophagy protects against liver fibrosis in mice. *Autophagy* **2015**, *11*, 1280–1292. [[CrossRef](#)] [[PubMed](#)]
30. Wan, J.; Benkdane, M.; Teixeira-Clerc, F.; Bonnafous, S.; Louvet, A.; Lafdil, F.; Pecker, F.; Tran, A.; Gual, P.; Mallat, A.; et al. M2 Kupffer cells promote M1 Kupffer cell apoptosis: A protective mechanism against alcoholic and nonalcoholic fatty liver disease. *Hepatology* **2014**, *59*, 130–142. [[CrossRef](#)] [[PubMed](#)]

31. Weiss, E.; Rautou, P.E.; Fasseu, M.; Giabicani, M.; de Chambrun, M.; Wan, J.; Minsart, C.; Gustot, T.; Couvineau, A.; Maiwall, R.; et al. Type I interferon signaling in systemic immune cells from patients with alcoholic cirrhosis and its association with outcome. *J. Hepatol.* **2017**, *66*, 930–941. [[CrossRef](#)]
32. Habib, A.; Creminon, C.; Frobert, Y.; Grassi, J.; Pradelles, P.; Maclouf, J. Demonstration of an inducible cyclooxygenase in human endothelial cells using antibodies raised against the carboxyl-terminal region of the cyclooxygenase-2. *J. Biol. Chem.* **1993**, *268*, 23448–23454. [[CrossRef](#)] [[PubMed](#)]
33. Eligini, S.; Habib, A.; Leuret, M.; Creminon, C.; Levy-Toledano, S.; Maclouf, J. Induction of cyclo-oxygenase-2 in human endothelial cells by SIN-1 in the absence of prostaglandin production. *Br. J. Pharmacol.* **2001**, *133*, 1163–1171. [[CrossRef](#)]
34. Khanam, H.; Shamsuzzaman. Bioactive Benzofuran derivatives: A review. *Eur. J. Med. Chem.* **2015**, *97*, 483–504. [[CrossRef](#)] [[PubMed](#)]
35. Shah, P.; Westwell, A.D. The role of fluorine in medicinal chemistry. *J. Enzym. Inhib. Med. Chem.* **2007**, *22*, 527–540. [[CrossRef](#)] [[PubMed](#)]
36. Lim, S.Y.; Yuzhalin, A.E.; Gordon-Weeks, A.N.; Muschel, R.J. Targeting the CCL2-CCR2 signaling axis in cancer metastasis. *Oncotarget* **2016**, *7*, 28697–28710. [[CrossRef](#)]
37. Rahman, M.; Selvarajan, K.; Hasan, M.R.; Chan, A.P.; Jin, C.; Kim, J.; Chan, S.K.; Le, N.D.; Kim, Y.B.; Tai, I.T. Inhibition of COX-2 in colon cancer modulates tumor growth and MDR-1 expression to enhance tumor regression in therapy-refractory cancers in vivo. *Neoplasia* **2012**, *14*, 624–633. [[CrossRef](#)]
38. Sobolewski, C.; Cerella, C.; Dicato, M.; Ghibelli, L.; Diederich, M. The role of cyclooxygenase-2 in cell proliferation and cell death in human malignancies. *Int. J. Cell Biol.* **2010**, *2010*, 215158. [[CrossRef](#)]

Disclaimer/Publisher's Note: The statements, opinions and data contained in all publications are solely those of the individual author(s) and contributor(s) and not of MDPI and/or the editor(s). MDPI and/or the editor(s) disclaim responsibility for any injury to people or property resulting from any ideas, methods, instructions or products referred to in the content.